

Exciton scattering and the dephasing of ESR and optical absorption lines: The 1,2,4,5-tetrachlorobenzene triplet exciton problem

R. D. Wieting^{a)} and M. D. Fayer^{b)}

Department of Chemistry, Stanford University, Stanford, California 94305

(Received 6 August 1979; accepted 28 September 1979)

The relationship between exciton scattering induced dephasing of the ESR and the optical transitions of triplet exciton bands is examined by properly including exchange in the line shape formalism. First, a simple heuristic model demonstrates that while the optical dephasing time can be associated with the exciton scattering rate, the ESR dephasing time is more closely associated with the distribution of final states in the scattering process. The full exchange problem is then examined and a formal solution is obtained for the low power steady state ESR spectrum. Application to the 1,2,4,5-tetrachlorobenzene triplet exciton system shows that the exciton ESR spectrum with its associated 1 μ sec dephasing time can be reproduced using a 20 psec exciton scattering rate obtained from the optical dephasing time. Exciton scattering occurs to a small region of k space ($\sim 5\%$ of the band) surrounding the initial k state. These results resolve the apparent conflict between the optical and ESR spectra in this system and indicate that exciton transport, while not strictly coherent, is nonetheless predominantly wavelike in character.

I. INTRODUCTION

The nature of exciton migration on a molecular scale and the degree of coherence in the transport process are subjects of vigorous investigation and debate. For Frenkel excitons¹ a fundamental question concerns the time scale on which the exciton will remain in a wave vector state $|k\rangle$. If scattering from an initial state $|k\rangle$ to a new state $|k'\rangle$ is fast and Markovian,² an exciton wave packet's group velocity fluctuates rapidly on the time scale of intermolecular motion and the transport occurs as a random walk between lattice sites. In the limit of slow scattering, the initial state $|k\rangle$ persists on a time scale long compared to intermolecular motion and transport has a wave-like component.

The dynamics of exciton scattering have been probed by a variety of spectroscopic techniques. The triplet exciton system in 1,2,4,5-tetrachlorobenzene (TCB) single crystals has been particularly intensively studied at liquid helium temperatures. In ESR investigations of triplet spin sublevel exciton band-to-band transitions in TCB, a dephasing time of approximately 1 μ sec was obtained, independent of the band state $|k\rangle$.³⁻⁵ In these studies the dephasing time was taken to imply that TCB is in the coherent limit at low temperatures. However, high resolution optical absorption measurements on the same system⁶ appeared to contradict these conclusions. In those experiments the optically accessible $k=0$ triplet exciton band transition was found to dephase in ~ 20 psec, implying a scattering rate 4 to 5 orders of magnitude faster than that determined by ESR techniques. Although some degree of coherence is indicated by the optical work, the question of the detailed nature of exciton transport in this system can only be answered by resolving the apparent conflict between the optical and ESR experiments.

The resolution can be found in a careful analysis of

the relationship between exciton scattering and spectroscopic dephasing times. Exchange of a species between two different states, or environments, causes the superposition associated with the spectral transition under observation to dephase, broadening the transition linewidth. This effect is well known from the classic example of the exchange of a spin between environments in which it has different resonance frequencies.⁷ The broadening of the observed line shape is a combined function of the exchange (scattering) rate, the rate of return to the initial state, and the difference in Larmor frequency of the spin transition in the two states.

An exciton system is a generalization of the two-state case to N states. In the former, each state forms an environment for the transition which is characterized by a unique resonance frequency. In an exciton band each state $|k\rangle$ is also characterized by a unique resonance frequency ω_k^0 . If a low-power applied field is used to probe the transition, then this type of system is equivalent to N independent two-level systems interacting only through exchange. Dephasing of a transition in any state $|k\rangle$ is likewise a combined function of the rates of scattering to $|k'\rangle$, the time for return to $|k\rangle$, and the differences in Larmor frequency for the transition in the different band states. The form of the scattering, given by the probability distribution of final states $|k'\rangle$ following scattering from $|k\rangle$, is as important as the overall rate of leaving $|k\rangle$. Thus, the dephasing time may be quite different from the scattering time.

In the following we shall present a two-part model of the dephasing of spectroscopic transitions by exciton scattering, and we shall use it to analyze the TCB triplet exciton system. The first part employs an analytically tractable heuristic representation of an exciton band which permits direct insight into the problem. It is shown that the dephasing of optical transitions yields the exciton scattering rate and that, in contrast, ESR dephasing times do not reflect the rate of scattering but rather are more closely related to the distribution of final states in the scattering event. In the second part the full exciton band is treated in the limit of a low-

^{a)}Permanent address: Research Laboratories, Eastman Kodak Company, Rochester, NY 14650.

^{b)}Alfred P. Sloan and Dreyfus Foundation Fellow.

power steady-state applied field and the complete exchange equations are formally solved for any distribution of final states in the scattering between band states. These results permit the quantitative calculation via numerical methods of the steady-state spectral line shape and the direct comparison of experiment with theory.

Applied to the TCB exciton system, this analysis identified the exciton scattering time with the optical dephasing time of 20 psec. The steady-state ESR experimental line shape is reproduced with excellent agreement for several different forms of the exciton scattering distribution. However, only in the case that exciton scattering occurs primarily to nearby $|k\rangle$ states is this theoretical agreement consistent with the 20-psec optical dephasing time and a reasonable number of states in the TCB exciton band. This result is in accord with independent stimulated spin-echo measurements on this system which indicate that spectral diffusion occurs over a few percent of the total bandwidth.³

A detailed description of exciton transport in TCB emerges from these results. Exciton scattering occurs with high frequency, but each scattering event results in only a small change in the exciton wave vector. While not in the strict coherent limit, transport in this system is essentially wavelike.

II. EXCITON SCATTERING AND SPECTRAL DEPHASING

A. Heuristic model

In an exciton system with interactions along only one crystallographic axis (e.g., TCB), the wave vectors k lie on a one-dimensional periodic (inverse) lattice, i.e., a ring. Stochastic exciton scattering can be represented as a random walk on the k -space ring, where a change in the exciton state is represented by a step to a new (not necessarily adjacent) ring site. A fundamental theorem of random walks states that in a walk with a mean step rate k_s on a ring of N sites, the mean rate of return to the initial site is $k_B = k_s/N$, independent of the form of the walk.⁸ Thus, an exciton initially in $|k\rangle$ which is scattered to other band states $|k'\rangle$ at rate k_s will return to $|k\rangle$ at rate k_B . This suggests a simple model for the dephasing of exciton band transitions.

Consider the exchange of an excitation between a pair of two-level systems $|S\rangle$ and $|B\rangle$. The system $|S\rangle$ represents a single exciton band state $|k\rangle$. The system $|B\rangle$ is a "bath" which represents the remaining $N-1$ states $|k'\rangle$ of the band which exchange population with $|k\rangle$. The transition frequency is ω_0 in $|S\rangle$ but is $\omega_0 + \Delta$ in $|B\rangle$, where Δ measures the average shift in Larmor frequency experienced during the time of residence in the bath. As discussed above, stochastic scattering from $|S\rangle$ with rate constant k_s implies that the rate constant for return from $|B\rangle$ will be $k_B = k_s/N$. Equilibrium of population between the state and the bath thus requires a bath population of N for unit population of $|S\rangle$.

We shall employ the Feynman, Vernon, and Hellwarth (FVH) geometrical representation of the density-matrix equation.⁹ Viewed in a frame rotating¹⁰ at the frequency

ω of the applied field the components of a pseudospin vector $\mathbf{r} = (r_1, r_2, r_3)$ contain linear combinations of the elements of the density matrix. The in-plane components r_1 and r_2 are equivalent to the in-plane magnetization of a spin system.

Consider the dephasing of $|S\rangle$ in the following gedanken. The experiment begins with an applied pulse of sufficient power to rapidly establish an in-plane component and then the field remains off. With the field applied at $\omega = \omega_0$ and along I in a frame rotating at ω , the initial conditions become $r_2^S(0) = 1$ and $r_2^B(0) = N$, with all other components equal to zero. Since the applied field is zero for $t > 0$, the in-plane components become decoupled from the out-of-plane (population) components which may then be neglected. The equations of motion are

$$\dot{r}_1^S = -k_s r_1^S + k_B r_1^B, \quad (1a)$$

$$\dot{r}_1^B = +k_s r_1^S - k_B r_1^B - \Delta r_2^B, \quad (1b)$$

$$\dot{r}_2^S = -k_s r_2^S + k_B r_2^B, \quad (1c)$$

$$\dot{r}_2^B = +\Delta r_1^B + k_s r_2^S - k_B r_2^B. \quad (1d)$$

For an exciton band $N \gg 1$, so $k_s \gg k_B$. With this condition, Eq. (1) may be solved subject to the initial conditions. We focus on the time dependence of the Π component of $|S\rangle$, $r_2^S(t)$. The decay of this initially prepared component yields the rate of phase loss in the state $|S\rangle$ via exchange. The general result is

$$r_2^S(t) = \frac{1}{D} \{ [\Delta^2(k_s^2 + \Delta^2) + k_s^2 k_B] e^{-k_s t} + k_s (k_s^2 + k_s k_B + \Delta^2) \times [(k_s + k_B) \cos \Delta t + \Delta \sin \Delta t] \}, \quad (2)$$

where

$$D = (k_s^2 + \Delta^2)^2 + k_s k_B (2k_s^2 + k_s k_B + 2\Delta^2)$$

and $k_s \gg k_B$. Two special cases of the greatest interest are discussed below.

When the shift in Larmor frequencies Δ is much greater than the scattering rate, i.e., $\Delta \gg k_s$, Eq. (2) reduces to an extremely simple form:

$$r_2^S(t) = e^{-k_s t}. \quad (3)$$

This result means that the superposition is completely dephased by the change of environment before it can return to the initial state, and the phase loss thus occurs simply with the scattering rate. This limit can be found in optical transitions where Δ is on the order of the exciton bandwidth, typically 10^{10} – 10^{12} Hz in triplet systems. Thus, optical spectra have a straightforward interpretation:

$$T_2^{\text{opt}} = 1/k_s. \quad (4)$$

If $\Delta \approx k_s$, dephasing occurs on a similar time scale.

When the scattering rate is much greater than the Larmor shift, i.e., $k_s \gg \Delta$, a more complicated expression is obtained,

$$r_2^S(t) = \cos \Delta t + \frac{\Delta}{k_s} \sin \Delta t + \frac{\Delta^2}{k_s^2} e^{-k_s t}. \quad (5)$$

The oscillatory behavior is an artifact of the oversimplified choice of a single resonance frequency $\omega_0 + \Delta$ for

the bath. In order to more realistically model scattering in an exciton band, an average over a distribution of frequencies $\{\Delta\}$ should be taken, reflecting the average distribution of states $|k'\rangle$ occupied during exchange. A variety of distributions are plausible depending upon the form of scattering. A reasonable choice is a Gaussian function centered on the initial state, as might result from scattering only to nearby states. If this distribution ranges over only a small fraction of the band, an average over frequency yields

$$r_2^S(t) = e^{-(Et)^2/2}, \quad (6)$$

where E is the standard deviation of $\{\Delta\}$. The limit $k_S \gg \Delta$ is applicable in ESR band-to-band transitions, where the exciton band dispersion is mirrored but greatly reduced.^{4(a)} T_2^{ESR} cannot be obtained directly from this result. However, since the ESR linewidth, i. e., the effective bandwidth, $B_E > E$, it is evident that dephasing of an ESR transition will occur on a time scale of B_E^{-1} or longer. These results suggest that T_2^{ESR} values measured in the $k_S \gg \Delta$ limit reflect the frequency spread of states involved in the exchange rather than the scattering rate between them.

B. Full-exchange problem

The preceding heuristic model permits qualitative insights by reducing the problem to the elementary one of exchange between two different environments. In the following, quantitative results are derived from a treatment of the full exciton band exchange problem. Exchange of an excitation between N independent two-level systems will be considered, where each system corresponds to a distinct exciton band state $|k\rangle$. A solution for the steady-state low-power spectrum is obtained.

Again we employ the FVH representation.⁹ Since a low-power coupling field is assumed, the population components r_3 are decoupled from the in-plane components and are constants proportional to the populations of the corresponding states. With an applied field at frequency ω along the I axis in the rotating frame, the sum of the r_2 components of the N states yields the absorption at that frequency.¹⁰ The equations of motion for $|m\rangle$, with resonance frequency ω_0^m , are

$$\dot{r}_1^m = -\Delta\omega^m r_2^m - \left[\sum_{j=1}^{N'} k_{mj} \right] r_1^m + \sum_{j=1}^{N'} k_{jm} r_1^j, \quad (7a)$$

$$\dot{r}_2^m = -\omega_1 r_3^m + \Delta\omega^m r_1^m - \left[\sum_{j=1}^{N'} k_{mj} \right] r_2^m + \sum_{j=1}^{N'} k_{jm} r_2^j, \quad (7b)$$

where the prime means that the $j = m$ term is excluded from the sums. The rate constant for scattering from $|m\rangle$ to $|j\rangle$ is k_{mj} , $\Delta\omega^m = \omega - \omega_0^m$, and r_3^m is the steady-state value of r_3^m , proportional to the equilibrium population of $|m\rangle$. Equation (7) expresses just the m th pair of N pairs of equations. Defining the sum of rate constants in the "loss" terms as

$$k_{mm} = - \sum_{j=1}^{N'} k_{mj}, \quad (8)$$

the full set of $2N$ equations can be compactly written in matrix form,

$$\dot{r}_1 = -\Delta\omega r_2 + K^T r_1, \quad (9a)$$

$$\dot{r}_2 = -\omega_1 r_3^0 + \Delta\omega r_1 + K^T r_2, \quad (9b)$$

where K^T is the transpose of the scattering matrix K . The m th elements of the column vectors r_1 , r_2 , and r_3^0 are r_1^m , r_2^m , and r_3^m , respectively, and the matrix $\Delta\omega$ is diagonal with m th diagonal element $\Delta\omega_0^m$.

The central term in these equations is the scattering matrix K , whose elements k_{mj} embody a complete description of the exciton scattering process. For each state $|m\rangle$ the associated diagonal element k_{mm} measures the total rate of loss from $|m\rangle$ via all scattering paths. From the discussion surrounding Eq. (4), we associate this total loss rate with the optical dephasing time of the state in question, i. e., $k_{mm} = -1/T_2^{\text{opt}}(m)$.

The specific form of any given scattering process determines the value of the off-diagonal elements. Exciton scattering may occur exclusively to states which are nearly isoenergetic with the initial state or to a broad distribution. At one extreme is the limit of scattering to nearest-neighbor states only. In this situation $k_{mj} = \frac{1}{2} k_S$ for $j = m \pm 1$ and zero for all other $j \neq m$. At the opposite extreme scattering to all states is equally probable, i. e., $k_{mj} = [1/(N-1)] k_S$ for all $j \neq m$.

Scattering in real exciton systems probably lies intermediate to these two extremes. A useful model employs a distribution in which the scattering rate falls off exponentially as the difference in wave vector between final and initial state increases, i. e., $k_{mj} = \kappa \exp[-D(m,j)/R]$ where κ is a normalized rate constant chosen so that scattering into any $|j\rangle$ equals scattering out of $|j\rangle$. Since an exciton band has periodic boundary conditions, the wave vector difference $D(m,j) = |m-j|$ when $|m-j| \leq \frac{1}{2}N$, but $D(m,j) = N - |m-j|$ when $|m-j| > \frac{1}{2}N$. The parameter R is equal to the "average range" of a scattering event and characterizes the width of the exponential distribution, which can be continuously varied between the two limits discussed above. Thus, while arbitrary, this form will provide an instructive means of considering intermediate situations.

Equation (9) can be formally solved in steady state for r_2 to yield

$$r_2(\omega) = \omega_1 [\Delta\omega + K^T \Delta\omega^{-1} K^T]^{-1} [K^T \Delta\omega^{-1}] r_3^0. \quad (10)$$

The absorption spectrum may then be calculated by evaluating the sum of the elements of Eq. (10) at a range of frequencies.

III. APPLICATION TO TRIPLET EXCITONS IN 1,2,4,5-TETRACHLOROBENZENE

In order to apply Eq. (10) to a calculation of the TCB triplet exciton ESR spectrum, the elements of $\Delta\omega$, r_3^0 , and K must be evaluated. It is first necessary to know the number of states which comprise the exciton band, for the value of N sets the dimensionality of the matrix calculation. This number is equivalent to the mean number of molecules lying in a one-dimensional chain segment over which the excited states are not severely disrupted, suggesting that N will be of the order of the in-

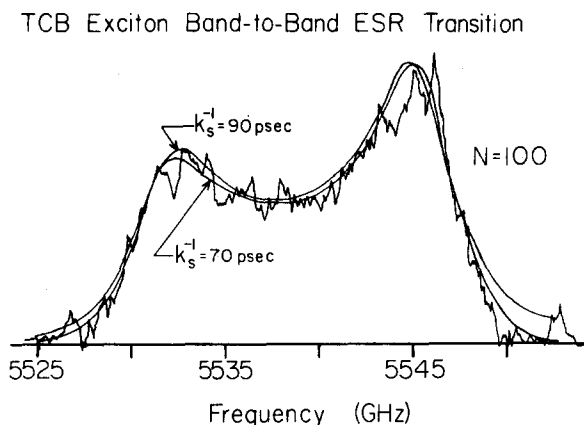


FIG. 1. The experimental ESR exciton band-to-band $|D| + |E|$ transition line shape for 1, 2, 4, 5-tetrachlorobenzene at 3.2°K (from Ref. 4). The theoretical curves were calculated from Eq. (10) using the nearest neighbor scattering distribution, with $N=100$. For this choice, best agreement was obtained with exciton scattering times $k_s^{-1} = 70$ to 90 psec (with the effective bandwidth $B_E = 18$ MHz). This figure illustrates that the experimental data can be reproduced using exciton scattering times in the picosecond range.

verse number density of chemical impurities or major lattice defects. Since residual major impurities may remain in this system in concentrations $\leq 10^{-3}$ – 10^{-4} mole mole, a rough estimate yields $N \sim 10^3$ – 10^4 .¹¹ N is also employed in the one-dimensional nearest-neighbor exciton band dispersion along with the effective bandwidth of the transition to evaluate the resonance frequencies ω_m^n of the states $|m\rangle$, which are used in $\Delta\omega$.

The population vector r_3^0 may be evaluated from the Boltzmann distribution in the band,^{4,5,12} Only this term contains the full bandwidth 4β and the experimental temperature.

Finally, the scattering rate and its form must be chosen and incorporated into K . As shown earlier in Sec. II, the rate constant for leaving $|m\rangle$ is equal to the inverse of the dephasing time of the optical transition, Only $|k=0\rangle$ is optically accessible from the ground state with $T_2^{\text{opt}} = 20$ psec, but, since the ESR dephasing times are independent of the band state, it seems plausible to assume the same behavior in the optical case. Thus, it remains only to choose a specific form of the scattering distribution, and the steady-state ESR line shape may be calculated for TCB. However, to perform the full numerical solution, it would be necessary to solve a system of simultaneous equations of order $N \sim 10^3$ – 10^4 . While possible in principle, it is more practical (and less costly) to perform the calculation for smaller values of N and to extrapolate the observed trends.

There are thus two variable parameters in the line-shape calculation: (i) the number of band states, N , and (ii) the ratio of the scattering rate to the effective bandwidth, k_s/B_E . Given a specific choice of (i) and (ii), the ESR spectrum is calculated on a frequency scale calibrated in units of B_E . Comparison of the calculated to the experimental spectrum provides in effect a measurement of this quantity and thereby yields the absolute scattering rate used in the calculation. We will calculate the TCB

spectrum over a range of N , optimizing the agreement to experiment for each choice of N by varying the value of k_s/B_E and then plot the absolute scattering rates k_s vs N .

The optically detected ESR $|D| + |E|$ transition line shape in TCB was calculated for several different scattering models in the manner discussed above. Figure 1 displays the experimental spectrum, obtained at 3.2°K,⁴ along with a pair of theoretically calculated curves which were optimized to bracket the experimental data. The bracketing procedure allows us to place an error bar on each calculation. These curves were calculated using the nearest-neighbor ($\Delta k = \pm 1$) scattering limit, with $N=100$ and $k_s^{-1} = 70$ –90 psec. The agreement is excellent and typical of the fit obtained in all of the calculations. Figure 1 illustrates an important point. It is possible to reproduce the experimental data using exciton scattering times in the picosecond range when exchange is properly included.

A variety of scattering distributions was considered in the order of increasing "average range" of scattering, the models employed were (i) nearest neighbor; (ii) exponential, $R=5\%$ of the exciton band; (iii) exponential, $R=20\%$ of the exciton band; and (iv) Markovian, equal probability of scattering to any state in the band. For each of these models a set of calculations was performed in which k_s/B_E was optimized for $N=20, 50$, and 100. The relationships between these optimized scattering rates and the number of band states is shown in Fig. 2, a log-log plot of k_s^{-1} vs N . In each case the data fit a straight line with good precision, permitting extrapolation to large N . Consider the steepest line, labeled NN (for nearest neighbor). For a nearest neighbor scattering distribution, $N=20$ band states requires a 2 nsec scattering rate to fit the experimental ESR data, while $N=50$ requires 320 psec. As discussed above the high-resolution optical spectrum implies a 20-psec scattering rate for TCB at these temperatures. Extrapolating the nearest-neighbor line to the 20 psec scattering line shows that nearest-neighbor scattering requires $N \cong 200$, a number slightly below the possible range. Extrapolating the exponential $R=5\%$ distribution to the 20 psec scattering line yields $N \cong 40\,000$. This value of N falls in range consistent with experiment. In contrast, the longer ranged $R=20\%$ exponential distribution requires an enormously greater number of band states, $N \cong 10^{10}$, a value which is orders of magnitude too large to be consistent with experiment. Finally, in the Markovian scattering limit it is impossible altogether to reconcile the ESR spectrum and the 20-psec scattering rate.

The results of these calculations demonstrate that TCB triplet exciton scattering at liquid helium temperatures occurs primarily to nearly isoenergetic states. This conclusion is necessary to reconcile the optical and ESR experiments. Independent evidence also suggests this scattering behavior. In an elegant experiment Schmidt and co-workers,³ using stimulated spin-echo measurements, observed that frequency instabilities of different sizes occur at quite different rates. They inferred that spectral diffusion due to scattering of the exciton $|k\rangle$ states is limited to a few hundred kHz in a

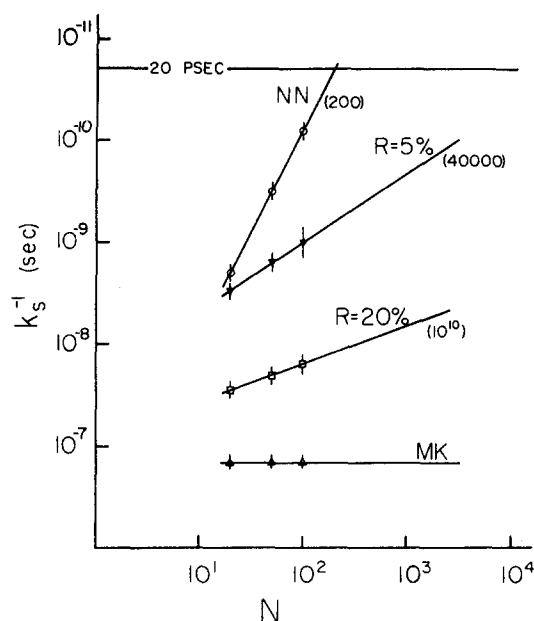


FIG. 2. The dependence of the exciton scattering rate k_s on the number of exciton band states N and on the distribution of final states in the scattering process, calculated via Eq. (10) for triplet excitons in 1, 2, 4, 5-tetrachlorobenzene at 3, 2°K. The four scattering distributions employed, in order of increasing width of the scattering distribution, were: nearest-neighbor scattering (NN); exponential ($R=5\%$ of band); exponential ($R=20\%$ of band); and Markovian (MK), equal probability of scattering to any final band state. For each model a linear log-log relationship is observed between k_s and N . The number in parentheses near each line is the value of N obtained from an extrapolation to $k_s^{-1}=20$ psec, the exciton scattering time obtained from optical-absorption experimental data (Ref. 5). The error bars reflect the uncertainty in the optimization to the experimental ESR spectrum, e.g., see Fig. 1.

total linewidth of about 10 MHz for the $|D|-|E|$ transition, or a few percent of the exciton bandwidth. Thus, the optical, ESR, and stimulated echo experiments combine with the exchange calculations presented here to give a detailed understanding of exciton scattering in the TCB system.

In summary, this analysis offers a resolution of the apparent conflict between the optical and ESR dephasing times which differ by orders of magnitude in TCB. Furthermore, it permits a semiquantitative determination of the exciton scattering distribution in this system.

These results show that exciton scattering is fast but that it occurs primarily to a small region of k space surrounding the initial state. In this situation the exciton group velocity undergoes small rapid fluctuations but is basically constant. Exciton migration in TCB at low temperature, while not strictly coherent, is nevertheless essentially wavelike.

ACKNOWLEDGMENTS

We would like to thank Professor W. G. Breiland, Department of Chemistry, University of Illinois at Urbana, for many informative conversations pertaining to this work. This work was supported in part by the National Science Foundation DMR Grant No. 76-22019 and acknowledgment is made to the Donors of the Petroleum Research Fund administered by the American Chemical Society for partial support of this research.

- ¹J. Frenkel, *Phys. Rev.* **37**, 17 (1931); **37**, 1276 (1931); A. S. Davydov, *Theory of Molecular Excitons* (Plenum, New York, 1971); in *Abstracts of the Eighth Molecular Crystal Symposium*, Santa Barbara, California, 1977 (unpublished).
- ²W. Feller, *An Introduction in Probability Theory and Its Applications* (Wiley, New York, 1966), Vols. I and II.
- ³B. J. Botter, A. I. M. Dicker, and J. J. Schmidt, *Mol. Phys.* **36**, 129 (1978).
- ⁴(a) A. H. Francis and C. B. Harris, *Chem. Phys. Lett.* **9**, 181 (1971); (b) **9**, 188 (1971).
- ⁵D. D. Dlott and M. D. Fayer, *Chem. Phys. Lett.* **41**, 305 (1976).
- ⁶D. M. Burland, D. E. Cooper, M. D. Fayer, and C. R. Gochanour, *Chem. Phys. Lett.* **52**, 279 (1977).
- ⁷H. M. McConnell, *J. Chem. Phys.* **28**, 430 (1958); T. J. Swift and R. E. Connick, *ibid.* **37**, 307 (1962); A. Carrington and A. D. McLachlan, *Introduction to Magnetic Resonance* (Harper and Row, New York, 1967).
- ⁸Katja Lakotos-Lindenberg and Kurt E. Schuler, *J. Math. Phys.* **12**, 633 (1971).
- ⁹R. P. Feynman, F. L. Vernon, Jr., and R. W. Hellwarth, *J. Appl. Phys.* **28**, 49 (1957).
- ¹⁰C. P. Slichter, *Principles of Magnetic Resonance* (Harper and Row, New York, 1963).
- ¹¹D. D. Dlott, M. D. Fayer, and R. D. Wieting, *J. Chem. Phys.*, **69**, 2752 (1978); W. Guettler, J. O. von Schuetz, and H. C. Wolf, *Chem. Phys.* **24**, 159 (1977); M. D. Fayer and C. B. Harris, *Phys. Rev. B* **9**, 748 (1974); R. M. Shelby, A. H. Zewail, and C. B. Harris, *J. Chem. Phys.* **64**, 3192 (1976).
- ¹²M. D. Fayer and C. B. Harris, *Phys. Rev. B* **9**, 748 (1974); C. B. Harris and M. D. Fayer, *ibid.* **10**, 1784 (1974).